ResNet Classifier Using Shearlet-Based Features for Detecting Change in Satellite Images

Emna Brahim[1], Sonia Bouzidi[1,2] and Walid Barhoumi[1,3]
[1]*Université de Tunis El Manar, Institut Supérieur d'Informatique d'El Manar, Research Team on Intelligent Systems in Imaging and Artificial Vision (SIIVA), LR16ES06 Laboratoire de Recherche en Informatique, Modélisation et Traitement de l'Information et de la Connaissance (LIMTIC), 2080 Ariana, Tunisia*
[2]*Université de Carthage, Institut National des Sciences Appliquées et de Technologie, 1080 Centre Urbain Nord BP Tunis Cedex, Tunisia*
[3]*Université de Carthage, Ecole Nationale d'Ingénieurs de Carthage, 45 Rue des Entrepreneurs, 2035 Tunis-Carthage, Tunisia*

Keywords: Change Detection, CNN, ResNet152, Shearlet Transform.

Abstract: In this paper, we present an effective method to extract the change in two optical remote-sensing images. The proposed method is mainly composed of the following steps. First, the two input Normalized Difference Vegetation Index (NDVI) images are smoothed using the Shearlet transform. Then, we used ResNet152 architecture in order to extract the final change detection image. We validated the performance of the proposed method on three challenging data illustrating the areas of Brazil, Virginia, and California. The experiments performed on 38416 patches showed that the suggested method has outperformed many relevant state-of-the-art works with an accuracy of 99.50%.

1 INTRODUCTION

In this work, we deal with the detection of the change in two remote sensing images acquired in the same area and at different times. In fact, change detection in remote sensing images is used in many approaches: Classification based on difference, difference based on classification, or only classification. In this framework, deep learning is among the most efficient tools in remote sensing and image interpretation, and it has shown its effectiveness in several connected domains such as change detection (Brahim et al., 2021), image classification (Mittal et al., 2022), and object detection (Bortoloti et al., 2022). Within the context of the first approach (classification based on difference), there are many methods used in change detection in optical remote sensing images such as: (Shi et al., 2021) who utilized a Deeply Supervised Attention Metric-based Network (DSAMNet). This technique allowed the treatment of large amounts of data with a recorded accuracy rate of 93.69%. However, (Brahim et al., 2021) employed the same techniques introduced by (Shi et al., 2021), but the input data were the subtract of the preprocessing images. Then, the authors used the Convolutional Neural Network (CNN) to detect the change. This method gave better results for all types of data compared to those provided by (Shi et al., 2021). Likewise, (Zhang et al., 2020) generated the Resnet to determine the features of the two input images, before identifying the difference between them in order to detect the change. This method did not give a better result (=96%), compared to that employed by (Brahim et al., 2021), and this is mainly due to the fact that (Zhang et al., 2020) did not utilize a performant Resnet type. However, (Wang et al., 2022) used a dual-path denoising network (DPDNet). The authors generated the difference image to extract the labels. Subsequently, they utilized the difference image to extract the features and applied a supervised classifier to extract the change in the studied images. This method showed higher efficiency and provided better accuracies (=98, 50%) than those presented in (Shi et al., 2021), (Zhang et al., 2020), and (Chen et al., 2022) where a multiscale supervised fusion network (MSF-Net) was investigated in order to detect the change. In fact, despite the precise generation of the difference between the features, the detection of the change in the two input images is quite inaccurate. Indeed, the used network gave an accuracy equal to 71% to detect the change. Regarding the methods used in the second approach (difference based on classification), (Dong

Brahim, E., Bouzidi, S. and Barhoumi, W.
ResNet Classifier Using Shearlet-Based Features for Detecting Change in Satellite Images.
DOI: 10.5220/0011781200003417
In *Proceedings of the 18th International Joint Conference on Computer Vision, Imaging and Computer Graphics Theory and Applications (VISIGRAPP 2023) - Volume 4: VISAPP*, pages 427-434
ISBN: 978-989-758-634-7; ISSN: 2184-4321

et al., 2020) utilized the network DADNN to classify the two input images and generate the difference between the obtained results. Although the execution of this method was very complex, it gave a 96% satisfactory accuracy rate. But, (Seyd et al., 2022) used the DNN-Net deep neural network (DNN-Net). This network gave a 91.15% accuracy which is low compared to that provided by the methods used in the first approach because in the first approach when we generated the difference before the classification, the information about the two images was detailed. Regarding the methods applied in the last approach (Only classification), (Zhang et al., 2022) employed SMD-Net to detect the change in the two input images. This method gave a 97.15% accuracy result, which is not better than that provided by the first approach.In this paper, we try to ameliorate the efficiency of of the first approach technique proposed by (Brahim et al., 2021), through developing a more efficient method and determining the efficacity of the subtract features compared with the subtract of the two input images.

The method is applied following the two steps described below: Smoothing the two input NDVI images using the Shearlet transform decomposition and K-means. Then, detecting the binary change by using ResNet152 to detect the final change. This paper is organized as follows: Section 2 defines the suggested method. Section 3 presents the conducted experiments and illustrates the obtained results. Finally, Section 4 concludes the paper and presents some future perspectives.

2 PROPOSED METHOD

The proposed method is presented in (Figure 1). The Shearlet transform was used to smooth the two input images by dividing them into high and low frequencies. Then, classifying them using K-means and reconstructing them to obtain the two smoothed images. After that, ResNet152 was used to extract the final result of the change.

2.1 Shearlet Transform

The shearlet transform, which is the 2D-Multiscale Geometric Decomposition (MGD) employed to smooth the two input NDVI images and detect the low and high coefficients of the two input images. In 2 dimension ($\xi = (\xi_1, \xi_2) \in \widehat{R}^2$), the Shearlet transform represents a frequency domain with dilations using the following function:

$$\varphi_{j,s,k}(x) = a^{\frac{-3}{4}} \varphi[U_s^{-1} V_a^{-1}(x-k)] \qquad (1)$$

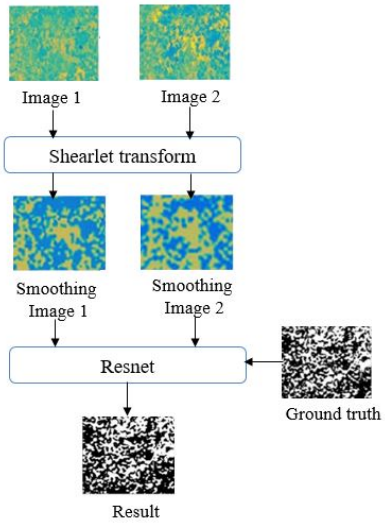

Figure 1: Flowchart of the proposed method.

Where $\varphi_{j,s,k}$ is a shearlet, j is the scale, $s \in R$ is the shear direction, k is the translation parameter, $V_a = \begin{pmatrix} a & 0 \\ a & \sqrt{a} \end{pmatrix}$ is the dilation matrix, $U_s = \begin{pmatrix} 1 & 1 \\ 0 & 1 \end{pmatrix}$ is the shear matrix, with a$\geq$ 0.

The coefficients were computed using several functions stated in the research work of (Brahim et al., 2021). The steps of image decomposition are as follows: First, applying the Laplacian Pyramid and directional filter to decompose the two images into low and high frequencies (Brahim et al., 2021) at scale j (Figure 2).

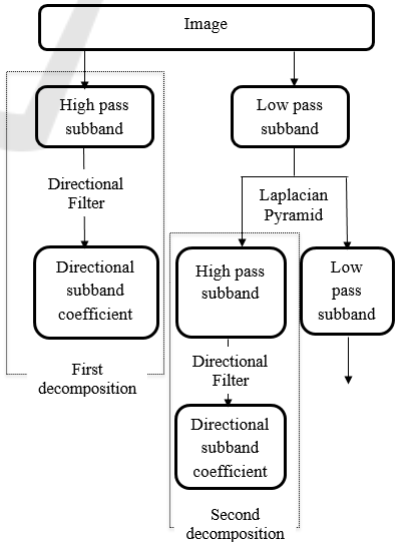

Figure 2: Exemple of illustration of the decomposition in two scales using Shearlet transform.

Classifying the low and high frequencies of each image and in each scale, using K-means with this al-

gorithm:

1. Identifying the number of clusters K. repeat (2, 3) when the cluster K does not change.
2. Assigning each coefficient to the closest partition.
3. updating the mean of each cluster.

After classifying the coefficient, we employed the inverse Fast Fourier Transform (FFT) to reconstruct the two smoothed input images.

Finally, ResNet152 was used to extract the binary change (0: Unchanged, 1: Changed) of the two smoothed images.

2.2 Residual Neural Network

The Residual neural network (ResNet152) includes several block layers and pooling layers used to detect the change (Figure 3).

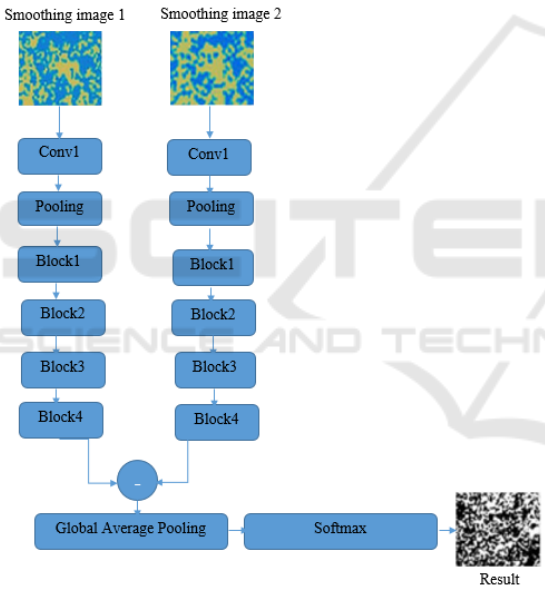

Figure 3: Flowchart of Resnet.

In fact, the adopted Resnet152 contains many convolutional layers. The first convolutional layer utilizes a kernel size equal to (5,5), while the other convolutional layers are composed of four blocks. Each block is made up of four convolutional layers having kernel sizes equal to (3,3) and the outputs of the channel in each block are respectively equal to 64, 128, 256, 512. After extracting the features of the first convolutional layers, the pooling layers were generated into (2, 2) sizes. Then, the four blocks were utilized to detect and subtract the features of the two images. Then, we generated the Average Pooling function into (2, 2). Finally, Softmax was used to detect the change in the two images.

3 RESULTS

In this section, we describe the data areas and the choice of the parameters of each technique applied in the introduced method. We also demonstrate and evaluate the obtained results and we show the efficiency of the developed method.

The treated data are multispectral NDVI images in order to facilitate the analysis and the treatment of the two images.

In the first data, the two images represented the region of Brazil having the following coordinates: (17 ° 10'S, 53 ° 10'N) and (19 ° 45'S, 55 ° 10'W). They were captured by the Landsat satellite between August 2000 and September 2001. The second data, are the two images representing the region of Virginia having the following coordinates: (31 ° 07'S, 23'N) and (081 ° 37'S, 44'W). They were captured by the Modis satellite between June 2021 and July 2022 and characterized by low spatial resolution. The third data, represent two images captured by Landsat satellite between March 2021 and April 2022. They show the region of California with the following coordinates: (34 ° 45'S, 29'N) and (084 ° 07'S, 51'W). The dimensions of the two images of the three data were 400×400. These images had low spatial resolution and were captured using two different satellites, as shown in Figure 4.

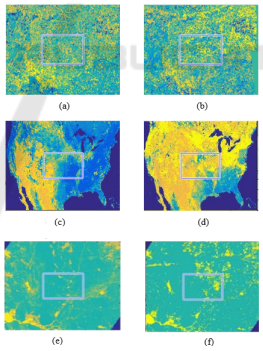

Figure 4: NDVI original images: (a) and (b) NDVI images captured in two periods 2000 and 2001. (c) and (d) NDVI images captured in two periods 2020 and 2021. (e) and (f) NDVI images captured in two periods 2021 and 2022.

The input original images were smoothed using the Shearlet transform. The latter has 5 scales and 5 orientations (0, 10, 10, 10,18), which allow the good smoothing of the two images. To show the high performance of the used Shearlet, a part of the two images (Figure 5) was framed and the Shearlet transform was decomposed. Then, the obtained coefficients were classified using k-means. The latter is better than the OTSU because it does not yield data loss. After classification, the inverse Shearlet was gener-

ated to reconstruct the two smoothed images in each data (Figure 5). To enhance the results given by the Shearlet transform, we examined an area framed in the two input images.

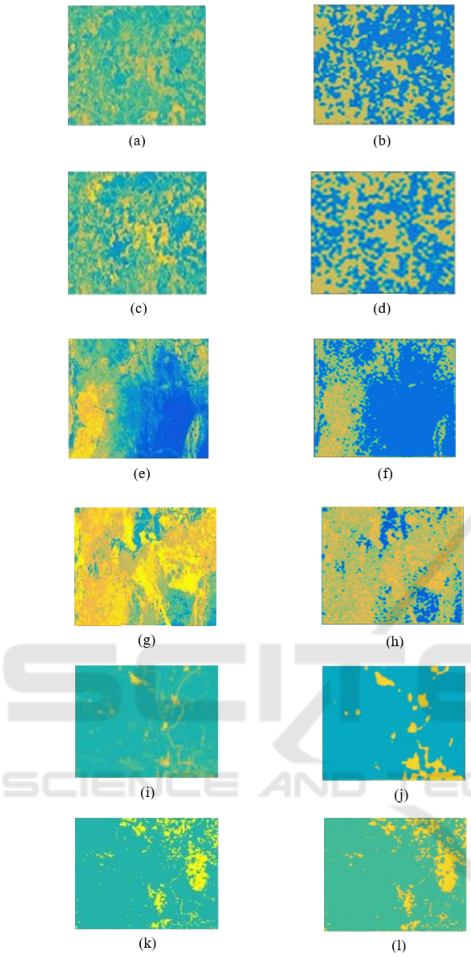

Figure 5: Smoothing area of the two images captured in August 2000 and September 2001 using Shearlet transform: (a) and (c) the area in August 2000 and September 2001, (b) and (d) Shearlet transform. (e) and (g) the area in June 2021 and July 2022, (f) and (h) shearlet transform. (i) and (k) the area captured in March 2021 and April 2022, (j) and (l) Shearlet transform.

Figure 5, shows that the smoothing of the images using Shearlet transform without employing other methods, such as Wavelet, etc., provided very satisfactory results. This method generated the multi-scale decomposition to smooth the images.

After smoothing, the two images were classified by ResNet152 using the CNN result of each pixel (changed or unchanged labels) as a ground truth. The convolutional neural network was employed to extract the labels. It contains nine convolutional layers where the first kernel size (3, 3) and other kernel sizes (5, 5) were used. CNN used the value 10 in the first channel because the studied data is an optical multispectral remote sensing. When we augmented the channel of the feature, the results became detailed. For the two first convolutional layers, the pooling function was transformed into (2, 2) size to extract the features. Then, the subtraction features and the three fully connected layers were determined to calculate the probability of the labels. Afterward, Softmax was applied to extract the labels in a binary form (0: Unchanged, 1: Changed). This classifier performed better than the others because it gave better classification results. The ground truth of the network CNN is the subtraction between the two smoothing input images. If the subtraction is equal to 0, the pixel is unchanged otherwise it is changed. The network was created using 200 epochs to detect the label of each pixel. In this step, we extracted in each data (Brazil, Virgina, California) a single area in each two input smoothing images with the same position which contains several changes in the ground truth. This area includes 38416 patches to better perceive the efficiency of the network. To evaluate our network, we tested three parameters: The training data, testing data, and the validation data. The three data are different. Concerning the training data, we used this data to know the hidden features of the network. However, we used the testing data to test the network after training. Then, the validation data was used to validate our proposed network. So, from the 38416 patches, we extracted (60% = 23050) in the training data, (20% = 7683) in the validation data, and (20% = 7683) in the testing data with the size (5, 5) for each patch.

The results obtained using CNN are the ground truth of the ResNet152 network. The latter was trained using the 'Adam' optimizer because it was the most widely used in the state of the art and gave good results. The findings provided by each data are illustrated in Figure 6, Figure 7, Figure 8, and Figure 9.

In Figure 6, the results illustrated in (A), (B), and (C) correspond to the labels of the two images in the three data. In fact, (a), (b), (c), and (d) represent respectively the first image, the second image, the benchmark, and the result of the CNN. The accuracy results obtained by the first, second, and third data were equal to 99.50%, 99.42%, and 99.46%, respectively. This network was validated using different types of data to validate the efficiency of the network by employing many convolutional layers to detect more details about the features. The second data was of Modis type, where the network gave the best results. The labels (changed and unchanged) of each pixel were determined by this network utilized in our previous work (Brahim et al., 2021). After this step,

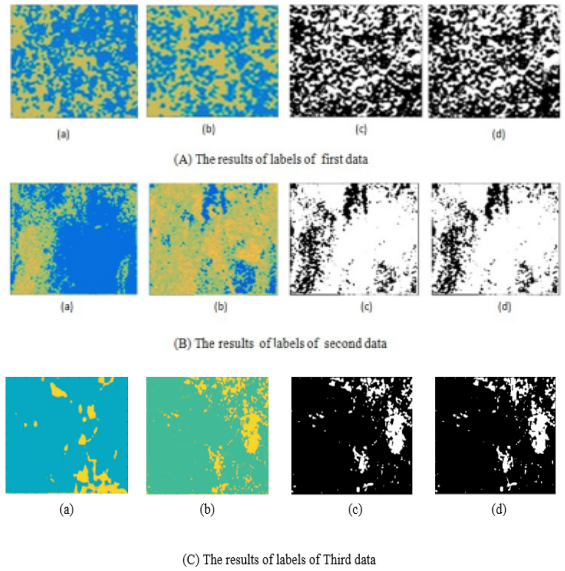

Figure 6: Extraction the labels of each data (Brazil, Virginia, California) using CNN where white and black pixels are respectively (Changed, Unchanged).

the results given by CNN were used in ResNet152. It showed high efficiency in detecting the final change using two smoothed images. Four layers were employed in this network (Resnet152), which contained blocks to demonstrate the features of these input images. Different values of kernel size of each convolutional layer were also obtained. The input kernel size, which was equal to 64 was chosen because it provided satisfactory results using the input multispectral optical images of the Resnet152 network. The latter was trained by the same optimizer and epochs of CNN. Then, the performance of the proposed method was validated by comparing it to that of the methods utilized by (Shi et al., 2021), (Brahim et al., 2021), (Zhang et al., 2020), (Dong et al., 2020), and (Chen et al., 2022) (Figure 7, 8 and 9). In each epoch, the accuracy and the loss were calculated and the parameters of this network were updated to improve the learning optimization.

In Figure 7, 8, and 9, the obtained results reveal that the findings provided by the suggested technique are better than those given by the other methods. The importance of the proposed method was observed in the subtraction between the features of the blocks in ResNet152 to detect the change and the network is made of several blocks of convolutional layers, which allow better detection of the change in the two images. When there were high features, the characteristics of each image were detailed and better classification findings were provided.

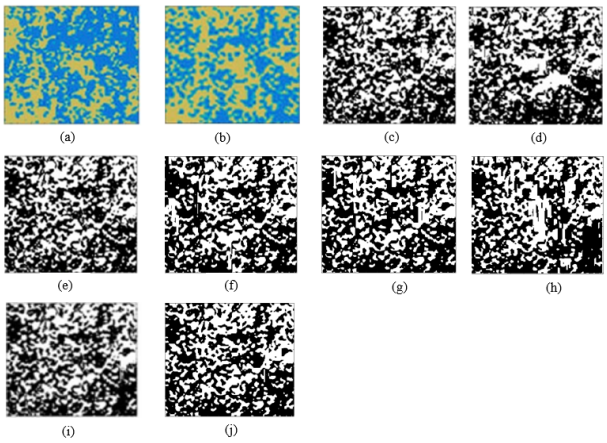

Figure 7: Change detection map results of Brazil data: (a), (b), (c), (d), (e), (f), (g), (h), (i), (j) represent respectively the first image, the second image, the ground truth, the results of the change detection of (Shi et al., 2021), (Brahim et al., 2021), (Zhang et al., 2020), (Dong et al., 2020), and (Chen et al., 2022), the method Shearlet+CNN, and the proposed method. Where white and black pixels are respectively (Changed, Unchanged).

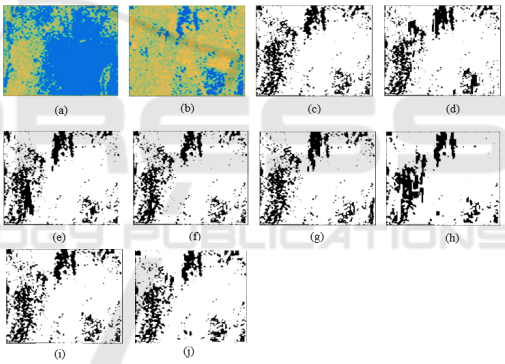

Figure 8: Change detection map results of Virgina data: (a), (b), (c), (d), (e), (f), (g), (h), (i), (j) represent respectively the first image, the second image, the ground truth, the results of the change detection of (Shi et al., 2021), (Brahim et al., 2021), (Zhang et al., 2020), (Dong et al., 2020), and (Chen et al., 2022), the method Shearlet+CNN, and the proposed method. Where white and black pixels are respectively (Changed, Unchanged).

The Recall, Accuracy, and F1-Score were computed using the following formula:

$$Recall = \frac{TP}{TP+FN} \tag{2}$$

$$Accuracy = \frac{(TP+TN)}{(TP+FN+TN+FP)} \tag{3}$$

$$F1-score = 2 \times \frac{(\frac{TP}{TP+FP}) \times Recall}{(\frac{TP}{TP+FP}) + Recall} \tag{4}$$

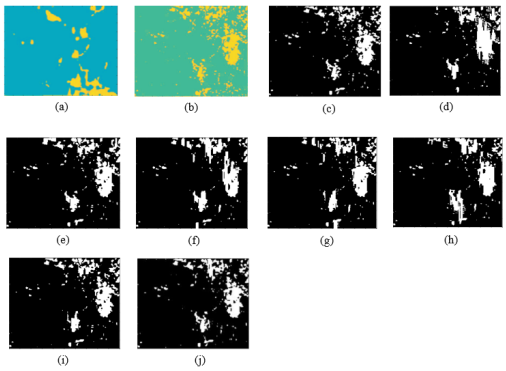

Figure 9: Change detection map results of California data: (a), (b), (c), (d), (e), (f), (g), (h), (i), (j) represent respectively the first image, the second image, the ground truth, the results of the change detection of (Shi et al., 2021), (Brahim et al., 2021), (Zhang et al., 2020), (Dong et al., 2020), and (Chen et al., 2022), the method Shearlet+CNN, and the proposed method. Where white and black pixels are respectively (Changed, Unchanged).

Where,TP, TN, FP and FN represent respectively true-positive, true-negative, false-positive and false-negative (Brahim et al., 2021). The data results are presented in Table 1 and the TP, TN, FP, FN are illustrated in Table 2.

In table 1, the difference values between the accuracy result given by our method and other existing methods in the first data are equal to 4.51%, 0.18%, 1.76%, 0.03%, 1.41%, and 5.2%, respectively. However, in the second data, the difference values are respectively equal to 2.52%, 0.29%, 1.7%, 0.05%, 1.39%, and 6.74%. As regards the third data, the difference values are respectively equal to 3.99%, 0.44%, 0.04%, 2.74%, 1.49%, and 3.75%. Using Table 1, we conclude that the value of the difference between the accuracy result given by the two methods DSAMNET (Shi et al., 2021), MSF-Net (Chen et al., 2022), and the proposed method in each data is important because in the two works (Shi et al., 2021) and (Chen et al., 2022) the input images were not preprocessed so the result of change detection was not better. For the two methods based on Shearlet+DI+CNN (Brahim et al., 2021) and Shearlet+CNN, the value of the difference between the accuracy result given by the two methods and the proposed method was low. However, in the first method based on Shearlet+DI+CNN (Brahim et al., 2021), the input data of the CNN were the subtraction of the two smoothed images using the Shearlet transform. In this shearlet, the authors used the OTSU to classify all the coefficients but in the second method, Shearlet+CNN, we utilized K-means to classify all the coefficients without losing the data and we generated the subtraction of the features for more convolutional layers of CNN. When the number of convolutional layers increases, the features become more detailed. So the result accuracy is increased compared to the result of Shearlet+DI+CNN (Brahim et al., 2021). The following Recall results obtained in the first and second data of MSF-Net (Chen et al., 2022) and DSAMNET (Shi et al., 2021) were low compared to the other methods and the proposed method with a value difference respectively equal to 5.17%, 0.34%, 0.89%, 0.18%, 0.67%, and 5.19% in the first data. In the second data, the value difference was respectively equal to 1.46%, 0.19%, 1.067%, 0.07%,0.85%, and 2.46%. In the third data, the following Recall results of Shearlet+DI+CNN (Brahim et al., 2021) was better compared to the proposed method because in the Shearlet+DI+CNN method (Brahim et al., 2021) the classifier of the coefficients in shearlet is OTSU so the data change can be lost. Then, The result of Shearlet+DI+CNN (Brahim et al., 2021) increased compared to the proposed method with a value equal to 0.4%, which is not a very important difference. The F1-score result in the first data, the second data and the third data was low compared to the proposed method. Obviously, the results improved the values, which were respectively equal, in the first data, to 5.05%, 0.17%, 0.9%, 0.01%, 0.44%, and 5.78%. In the second data, the difference values were respectively equal to 1.55%, 0.17%, 1.06%, 0.037%, 0.85%, and 2.83%. However, in the third data, they were equal to 17.05%, 2.59%,10.88%, 1.23%, 7.2%, and 15.58%. The accuracy result and the F1-score result of the proposed method increased compared to the result of method Shearlet+CNN. Therefore, The Resnet152 network played an important role in the change detection. Table 1 shows that, in each data, the accuracy result of the proposed method was considerably higher compared to that of the other methods.

In Table 2, the result of FN of the proposed method in the first data decreased compared to other methods. For example, the difference value provided by the method Shearlet+DI+CNN (Brahim et al., 2021) and the introduced method was equal to 0.35% in the first data, and equal to 0.19%, in the second data. However, in the third data, the FN result increased, because the Recall result of the Shearlet+DI+CNN method (Brahim et al., 2021) was superior to the Recall result of the proposed method. Consequently, the TP result of the Shearlet+DI+CNN method (Brahim et al., 2021) was important compared to the result of the proposed method. The degradation value was not important so the accuracy value of the proposed method was better. Using the proposed method, the FP result in three data was better and increased compared to the result of the proposed

Table 1: Change detection results obtained by the proposed method with those provided by some relevant methods applied in the state of the art (best values are in bold).

Data	Methods	Recall(%)	F1-score(%)	Accuracy(%)
Brazil	DSAMNET (Shi et al., 2021)	94.43	94.35	94.99
	Shearlet+DI+CNN (Brahim et al., 2021)	99.26	99.23	99.314
	ResNet (Zhang et al., 2020)	98.72	98.51	97.74
	Shearlet+Difference Features+Classifiers	99.43	99.40	99.47
	DADNN (Dong et al., 2020)	98.93	98.96	98.09
	MSF-Net (Chen et al., 2022)	94.42	93.63	94.26
	The proposed method	**99.61**	**99.41**	**99.50**
Virginia	DSAMNET (Shi et al., 2021)	98.30	98.09	96.90
	Shearlet+DI+CNN (Brahim et al., 2021)	99.57	99.47	99.13
	ResNet (Zhang et al., 2020)	98.69	98.57	97.72
	Shearlet+Difference Features+Classifiers	99.69	99.61	99.37
	DADNN (Dong et al., 2020)	98.91	98.79	98.03
	MSF-Net (Chen et al., 2022)	97.30	96.81	94.75
	The proposed method	**99.76**	**99.64**	**99.42**
California	DSAMNET (Shi et al., 2021)	83.87	81.78	95.50
	Shearlet+DI+CNN (Brahim et al., 2021)	**98.38**	96.24	99.05
	ResNet (Zhang et al., 2020)	87.90	87.95	96.75
	Shearlet+Difference Features+Classifiers	98.21	97.60	99.46
	DADNN (Dong et al., 2020)	93.95	91.63	98.00
	MSF-Net (Chen et al., 2022)	84.37	83.25	95.74
	The proposed method	97.98	**98.83**	**99.49**

Table 2: Obtained TN, FP, FN, and TP rates given by the proposed method, CNN without Shearlet and SCNN (best values are in bold).

Data	Methods	TN(%)	FP(%)	FN(%)	TP(%)
Brazil	DSAMNET (Shi et al., 2021)	95.44	4.55	5.5	94.43
	Shearlet+DI+CNN (Brahim et al., 2021)	99.35	0.64	0.73	99.26
	ResNet (Zhang et al., 2020)	93.45	6.5	1.3	98.69
	Shearlet+CNN	99.49	0.5	0.56	99.43
	DPDNET (Wang et al., 2022)	94.39	5.6	1	98.93
	MSF-Net (Chen et al., 2022)	94.10	5.8	5.5	94.42
	The proposed method	**99.38**	**0.61**	**0.38**	**99.61**
Virginia	DSAMNET (Shi et al., 2021)	90.90	9	1.6	98.30
	Shearlet+DI+CNN (Brahim et al., 2021)	97.27	2.7	0.42	99.57
	ResNet (Zhang et al., 2020)	93.24	6.7	1.2	98.72
	Shearlet+CNN	97.91	2.04	0.3	99.69
	DPDNET (Wang et al., 2022)	94.20	5.79	1	98.91
	MSF-Net (Chen et al., 2022)	81.87	18.12	2.6	97.30
	The proposed method	**97.99**	**2**	**0.23**	**99.76**
California	DSAMNET (Shi et al., 2021)	99.70	2.8	16	83.87
	Shearlet+DI+CNN (Brahim et al., 2021)	99.14	0.85	**1.6**	**98.38**
	ResNet (Zhang et al., 2020)	98.00	1.9	12	87.90
	Shearlet+CNN	99.61	0.38	1.7	98.21
	DPDNET (Wang et al., 2022)	98.57	14	6.04	93.95
	MSF-Net (Chen et al., 2022)	97.35	2.6	15	84.37
	The proposed method	**99.71**	**0.28**	2	97.98

method, because the TN result of the other methods was very low compared to the result of the proposed method. Accordingly, the FP result of the proposed method was better.

4 CONCLUSION AND PERSPECTIVES

In this work, we presented a method of change detection based on Shearlet transform, CNN and ResNet152. The Shearlet transform allowed decomposing the two input images into low and high frequencies. Then, reconstructing them to smooth the two input images. After that, the labels (changed, unchanged) were detected using the CNN network to use them in Resnet. Afterward, the ResNet was generated to extract the features using many blocks and generating their subtraction. Subsequently, the classifier was employed to detect the change. Despite its good results and high efficiency compared to the methods introduced in the first approach. This method is characterised by the shearlet and two networks where each networks is composed by many convolutional layers. As far as the shearlet transform is concerned, it allows to facilitate the treatement of the two input images. But, this method can cause problems in the treatment of the hyperspectral images.

Therefore, in future works, we will further explore our method to enhance our network or create other networks to detect the change variance.

REFERENCES

Bortoloti, F. D., Tavares, J., Rauber, T. W., Ciarelli, P. M., and Botelho, R. C. G. (2022). An annotated image database of building facades categorized into land uses for object detection using deep learning. Machine Vision and Applications, 33(5), 1-16.

Brahim, E., Bouzidi, S., and Barhoumi, W. (2021). Change detection in optical remote sensing images using shearlet transform and convolutional neural networks. In 2021 IEEE/ACS 18th International Conference on Computer Systems and Applications (AICCSA), (pp. 1-7).

Chen, J., Fan, J., Zhang, M., Zhou, Y., and Shen, C. (2022). MSF-Net: A Multiscale Supervised Fusion Network for Building Change Detection in High-Resolution Remote Sensing Images. IEEE Access, 10, 30925-30938.

Dong, H., Ma, W., Wu, Y., Zhang, J., and Jiao, L. (2020). Self-supervised representation learning for remote sensing image change detection based on temporal prediction. Remote Sensing, 12(11), 1868.

Han, M., Li, R., and Zhang, C. (2022). LWCDNet: A Lightweight Fully Convolution Network for Change Detection in Optical Remote Sensing Imagery. IEEE Geoscience and Remote Sensing Letters, 19, 1-5.

Li, X., Du, Z., Huang, Y., and Tan, Z.(2021). A deep translation (GAN) based change detection network for optical and SAR remote sensing images. ISPRS Journal of Photogrammetry and Remote Sensing, 179, 14-34.

Liu, M., Shi, Q., Liu, P., and Wan, C. (2020). Siamese Generative Adversarial Network for Change Detection Under Different Scales. In IGARSS 2020-2020 IEEE International Geoscience and Remote Sensing Symposium (pp. 2543-2546). IEEE.

Mittal, S., Srivastava, S., and Jayanth, J. P. (2022). A Survey of Deep Learning Techniques for Underwater Image Classification. IEEE Transactions on Neural Networks and Learning Systems.

Shi, Q., Liu, M., Li, S., Liu, X., Wang, F., and Zhang, L. (2021). A deeply supervised attention metric-based network and an open aerial image dataset for remote sensing change detection. IEEE Transactions on Geoscience and Remote Sensing, PP(99):1-16.

Shi, K., Bai, L., Wang, Z., Tong, X., Mulvenna, M. D., and Bond, R. R. (2022). Photovoltaic Installations Change Detection from Remote Sensing Images Using Deep Learning. In IGARSS IEEE International Geoscience and Remote Sensing Symposium (pp. 3231-3234).

Wang, J., Gao, F., Dong, J., Du, Q., and Li, H. C. (2022). Change Detection From Synthetic Aperture Radar Images via Dual Path Denoising Network. IEEE Journal of Selected Topics in Applied Earth Observations and Remote Sensing, 15, 2667-2680.

Zhang, H., Liu, J., and Xiao, L. (2020). Bipartite Residual Network for Change Detection in Heterogeneous Optical and Radar Images. In IGARSS IEEE International Geoscience and Remote Sensing Symposium (pp. 332-335).

Zhang, X., He, L., Qin, K., Dang, Q., Si, H., Tang, X., and Jiao, L. (2022). SMD-Net: Siamese Multi-Scale Difference-Enhancement Network for Change Detection in Remote Sensing. Remote Sensing, 14(7), 1580.